Journal of Neurochemistry

JOURNAL OF NEUROCHEMISTRY | 2010 | 112 | 854–869 doi: 10.1111/j.1471-4159.2009.06535.x

Intermittent hypoxia during sleep induces reactive gliosis and limited neuronal death in rats: implications for sleep apnea

Rolando Xavier Aviles-Reyes,*,[1] Maria Florencia Angelo,*,[1] Alejandro Villarreal,* Hugo Rios,* Alberto Lazarowski*,† and Alberto Javier Ramos*

*Instituto de Biología Celular y Neurociencia "Prof. E. De Robertis", Facultad de Medicina, Universidad de Buenos Aires, Calle Paraguay 2155 3er piso (1121), Ciudad de Buenos Aires, Argentina

†Departamento de Análisis Clínicos, Facultad de Farmacia y Bioquímica, Calle Junín 956 (1121), Ciudad de Buenos Aires, Argentina

Abstract

Sleep apnea (SA) can be effectively managed in humans but it is recognized that when left untreated, SA causes long-lasting changes in neuronal circuitry in the brain. Recent neuroimaging studies gave suggested that these neuronal changes are also present even in patients successfully treated for the acute effects of SA. The cellular mechanisms that account for these changes are not certain but animal models of intermittent hypoxia (IH) during sleep have shown neuronal death and impairment in learning and memory. Reactive gliosis has a drastic effect on neuronal survival and circuitry and in this study we examined the neuro-glial response in brain areas affected by SA. Glial and neuronal alterations were analyzed after 1, 3, 5 and 10 days of exposure to IH (8 h/day during the sleep phase, cycles of 6 min each, 10–21% O_2) and observed significant astroglial hyperplasia and hypertrophy in parietal brain cortex and hippocampus by studying gliofibrillary acidic protein, Vimentin, S100B and proliferating cell nuclear antigen expression. In addition, altered morphology, reduced dendrite branching and caspase activation were observed in the CA-1 hippocampal and cortical (layers IV–V) pyramidal neurons at short exposure times (1–3 days). Surprisingly, longer exposure to IH reduced the neuronal death rate and increased neuronal branching in the presence of persistent reactive gliosis. Up-regulation of hypoxia inducible factor 1 alpha (HIF-1α) and mdr-1, a HIF-1α target gene, were observed and increased expression of receptor for advanced end glycated products and its binding partner S100B were also noted. Our results show that a low number of hypoxic cycles induce reactive gliosis and neuronal death whereas continuous exposure to IH cycles reduced the rate of neuronal death and induced neuronal branching on surviving neurons. We hypothesize that HIF-1α and S100B glial factor may improve neuronal survival under hypoxic conditions and propose that the death/survival/re-growth process observed here may underlie brain circuitry changes in humans with SA.

Keywords: glia, HIF, hypoxia, RAGE, reactive gliosis, S100B, sleep apnea.

J. Neurochem. (2010) **112**, 854–869.

Sleep apnea syndrome (SA) is a very common pathology in adult humans. SA patients suffer a repeated and transient reduction in oxygen tension termed intermittent hypoxia (IH). The CNS is vulnerable to these hypoxic conditions and neurocognitive manifestations of SA include not only daytime sleepiness, but also alterations in personality, impairment of concentration, perception, memory, communication and learning (Engleman *et al.* 2000; Décary *et al.* 2000; Gozal and Kheirandish-Gozal 2007, 2008; Roure *et al.* 2008). Continuous positive airway pressure therapy reduces daytime sleepiness and cardiovascular complications of SA (Basner 2007). However, even in patients using continuous positive airway pressure therapy, executive dysfunction often persists and this may reflect structural and functional

Received August 31, 2009; revised manuscript received November 2, 2009; accepted November 10, 2009.

Address correspondence and reprint requests to Alberto Javier Ramos, Laboratorio de Neuropatología Molecular, Instituto de Biología Celular y Neurociencia "Prof. E. De Robertis", Facultad de Medicina, Universidad de Buenos Aires, Calle Paraguay 2155 3er piso, (1121) Ciudad de Buenos Aires, Argentina. E-mail: jramos@fmed.uba.ar

[1]These authors contributed equally to this study.

Abbreviations used: DG, dentate gyrus; FLICA, FAM-VAD-FMK, carboxyfluorescein-labeled fluoromethyl ketone peptide; GFAP, gliofibrillary acidic protein; HIF-1α, hypoxia inducible factor 1 alpha; IH, intermittent hypoxia; MAP-2, microtubule associated protein 2; MDR-1, multidrug resistance protein 1; NeuN, anti-neuronal nuclei; NFκB, nuclear factor kappa B; PCNA, proliferating cell nuclear antigen; RAGE, receptor for advanced end glycated products; ROD, relative optical density; SA, sleep apnea syndrome; SVZ, subventricular zone.

alterations in brain neurocircuitry (Thomas *et al.* 2005; Naegele *et al.* 1998; Feuerstein *et al.* 1997).

Several experimental paradigms have suggested that neuronal alterations are the main reason for cognitive deficits observed in animal models and human patients (Gozal *et al.* 2001, 2003; Row *et al.* 2002; Xu *et al.* 2004; Altay *et al.* 2004; Machaalani and Waters 2003; Pae *et al.* 2005; Zhu *et al.* 2008). Major cognitive impairments are functionally related to changes in hippocampal and cortical areas, especially the CA1 region of the hippocampus and layers IV and V of the cortex (Gozal *et al.* 2001, 2002; Row *et al.* 2003; Payne *et al.* 2004; Hung *et al.* 2008; Sizonenko *et al.* 2003). Consistent with this, human SA patients have shown a reduction in gray matter content (Morrell and Twigg 2006; Ayalon and Peterson 2007). The precise mechanisms that lead to neuronal changes in SA are not known but production of reactive oxygen species during the reoxygenation period (reviewed in Lavie 2003), glutamate-induced excitotoxicity (Fung *et al.* 2007) and inflammation (Bravo *et al.* 2007; Burckhardt *et al.* 2008) have all been implicated in the development of the neuronal pathology.

Astrocytes are crucial participants in many aspects of normal CNS. In disease states, astrocytes undergo complex phenotypic changes, generically referred as reactive gliosis (reviewed in Ridet *et al.* 1997; Maragakis and Rothstein 2006). Reactive gliosis was originally considered to reduce neuronal survival after brain injury because reactive astrocytes secrete pro-inflammatory cytokines, produce reactive oxygen species and nitric oxide, and form a glial scar that impedes neuronal reconnection. However, there is now abundant data showing that reactive astrocytes can promote the recovery of CNS function. Reactive astrocytes can produce energy substrates and trophic factors for neurons and oligodendrocytes, act as free radical and glutamate scavengers, actively restore the blood-brain barrier, promote neovascularization, restore CNS ionic homeostasis, promote remyelination and stimulate neurogenesis from neural stem cells (reviewed in Liberto *et al.* 2004; Privat 2003; Stoll *et al.* 1998). Reactive astrocytes also secrete S100B, the binding partner of the receptor for advanced end glycated products (RAGE), that is able to induce neuronal apoptosis or survival depending on the concentration (Huttunen *et al.* 2000; Donato 2003; Ramos *et al.* 2004; Gerlach *et al.* 2006).

Hypoxia exposure leads to the rapid activation of a transcription factor termed hypoxia inducible factor 1 alpha (HIF-1α). HIF-1α induces genes related to angiogenesis, erythropoiesis and energy metabolism that mediate adaptation to hypoxia (Sharp *et al.* 2001; Semenza 2002a,b; Sharp and Bernaudin 2004) including vascular endothelial growth factor, atrial natriuretic peptide, nitric oxide synthase, glucose transporter and glycolytic enzymes (Semenza 2002a,b). The expression of these genes improves cell survival at low oxygen levels and limits damage after a second hypoxic insult, a phenomenon known as pre-conditioning (see for review Bernhardt *et al.* 2007; Lu *et al.* 2005). HIF-1α is often regarded as the major transcription factor associated with hypoxia but experimental evidence suggests that nuclear factor kappa B (NFκB), activator protein 1, heat shock factor-1 and Sp1 (Sharp *et al.* 2001; Nanduri and Nanduri 2007) are also activated by hypoxia and play protective roles.

In an attempt to understand the early glial response to IH and to analyze how glial response may affect neuronal survival, in this report we followed the response of astrocytes and neurons after 1, 3, 5 or 10 days of exposure to cycles of IH. Prominent reactive gliosis and increased S100B expression was observed in astrocytes from brain cortex and hippocampus as well as activation of neuro-gliogenic niches in the dentate gyrus (DG) and subventricular zone (SVZ). Hippocampal and cortical pyramidal neurons showed shorter dendrites, altered nuclear morphology and activated caspases especially after 1 and 3 days of IH. Increased abundance of HIF-1α and RAGE expression was also observed in cortical and hippocampal pyramidal neurons. Surprisingly, most neuronal alterations were significantly reduced after 10 days of continuous exposure to IH while reactive gliosis persisted.

Materials and methods

Materials

Antibodies were obtained from Sigma, St Louis, MO, USA [microtubule associated protein 2 (MAP-2) Nf-200, Nf-68, S100B, proliferating cell nuclear antigen (PCNA), Vimentin], Upstate Biotechnology, Lake Placid, NY, USA (HIF-1α), Dako, Carpinteria, CA, USA (gliofibrillary acidic protein, GFAP; multidrug resistance protein 1, MDR-1), Iowa University Hybridoma Bank (Nestin) and Chemicon, Temecula, CA, USA (anti-neuronal nuclei, NeuN). Secondary biotinylated antibodies and streptavidin complex (Extravidin) used for immunohistochemistry studies were purchased from Sigma. Secondary fluorescent antibodies were obtained from Jackson Immunoresearch. Caspatag kit was purchased from Chemicon. All other chemical substances were of analytical grade. PCNA antibody was a gift of Dr. Alicia Brusco, University of Buenos Aires.

Animals

Adult male Wistar rats (250–300 g) from the animal facility of the School of Pharmacy and Biochemistry (University of Buenos Aires) were used in this study. Animals were housed in a controlled environment (12/12-h light/dark cycle, controlled humidity and temperature, free access to standard laboratory rat food and water). The animal care for this experimental protocol was in accordance with the NIH guidelines for the Care and Use of Laboratory Animals and the principles presented in the Guidelines for the Use of Animals in Neuroscience Research by the Society for Neuroscience.

Intermittent hypoxia exposure

Animals were randomly divided into five experimental groups and placed in two identical plastic normobaric chambers (capacity: 8 L) during the light period of the day. The groups were named IH-1, IH-3, IH-5 and IH-10, representing animals that have undergone

exposure to IH for 1, 3, 5 and 10 days. The gas mixture with the desired O_2 concentration was continuously flushed at a rate of 16 L/min to ensure two complete renewals of chamber air per minute. The O_2 level in each chamber was monitored continuously with an electrochemical sensor connected to a digital oxymeter (PumpControl, Buenos Aires, Argentina) and regulated by timer-controlled valves connected to room air and to a N_2 source equipped with separated flow mixers. Room air and N_2 were pre-mixed before entry to the chamber. The IH treatment was applied for 1, 3, 5 or 10 days, 8 h/day during the light phase. During this time O_2 was reduced from 21% to 10% over 1 min, held at 10% for 5 min, returned to 21% over 1 min, and held at 21% for 6 min. This cycle was repeated continuously for 8 h and gives a minimum of five hypoxic events per hour of sleep accordingly with the clinical definition of sleep apnea (Basner 2007) and to produce a mild IH-exposure paradigm. Control animals were housed in identical chambers for an equivalent amount of time, and were exposed to the same timer- and valve-controlled changes in air flow as the IH rats. However, the only source of gas in the control chambers was room air, so they remained at normoxic levels throughout the protocol. Immediately after hypoxia session, the cages were returned to the housing room. This protocol was adapted from previous literature (Ma *et al.* 2008; Ling *et al.* 2008; Klein *et al.* 2005; Hinojosa-Laborde and Mifflin 2005) and in our hands has been shown to decrease the rat's oxygen hemoglobin saturation by 15–20% and increase heart rate by 20–30 beats/min.

Fixation

Animals were deeply anaesthetized with chloral hydrate 300 mg/kg (i.p.) and were perfused through the left ventricle, initially with saline solution containing 5000 UI of heparin and subsequently with a fixative solution containing 4% w/v paraformaldehyde and 0.25% v/v glutaraldehyde in 0.1 M phosphate buffer, pH 7.2. Following the delivery of 300 mL of fixative solution through a peristaltic pump, brains were removed and kept in cold fixative solution for 90 min. Brains were then washed three times in cold 0.1 M phosphate buffer pH 7.4 containing 5% w/v sucrose, and left in wash solution for 18 h at 4°C. Brains were cryoprotected by immersing them in a solution containing 25% w/v sucrose in 0.1 M phosphate buffer pH 7.4 and stored at −20°C. Coronal 50-μm-thick brain sections were cut using a cryostat. The sections were cryoprotected by immersing them in a solution containing 20% of glycerol plus 30% of ethylene glycol in 0.1 M phosphate buffer pH 7.4 and stored at −20°C.

Immunohistochemistry

Brain sections of animals from experimental groups were simultaneously processed in the free floating state as previously described (Ramos *et al.* 2000, 2004; Angelo *et al.* 2009). After endogenous peroxidase activity inhibition, brain sections were permeabilized, unspecific binding blocked and the sections were incubated with primary antibodies with the indicated dilutions: GFAP 1 : 1000; HIF-1α 1 : 1000; S100B 1 : 800; MDR-1 1 : 1000; MAP-2 1 : 1000; Nf-200 1 : 1000; Nf-68 1 : 1000, NeuN 1 : 1000; PCNA 1 : 500; Vimentin 1 : 1000; Nestin 1 : 500. After 48 h incubation at 4°C, slices were rinsed and incubated with biotinylated secondary antibodies and extravidin complex. Development of peroxidase activity was carried out with 0.035% w/v 3,3′ diaminobenzidine plus 2.5% w/v nickel ammonium sulfate and 0.1% v/v H_2O_2 dissolved in acetate buffer 0.1 M pH 6.0. Controls for the immunohistochemistry procedure were routinely performed by omitting the primary antibody. These control sections did not develop any immunohistochemical labelling. Double fluorescent immunostaining studies were performed essentially in the same way but the endogenous peroxidase inhibition was omitted and isotypic specific secondary antibodies (Jackson Immuno-Research, West Grove, PA, USA) labelled with FITC or Rhodamine RRX were used in a 1 : 400 dilution. Photographs were taken in a Zeiss Axiophot microscope equipped with a digital camera (Olympus Q5, Olympus, Tokyo, Japan).

Active caspases detection

A different set of animals from IH groups were anaesthetized as stated before and decapitated. Brains were quickly dissected over ice and snap frozen at −70°C. Brain sections of 15 μm thick were obtained in cryostat, mounted on glass slides and kept at −70°C until use. The active caspase assay (Caspatag, Chemicon) was used as indicated by the supplier. This methodology is based on carboxyfluorescein-labeled fluoromethyl ketone peptide FLICA (FAM-VAD-FMK), a permeable and non-cytotoxic fluorochrome inhibitor of caspases that enters the cell and covalently binds to a reactive cysteine residue that resides on the large subunit of the active caspase heterodimer. Brain sections were incubated with the FLICA solution for 2 h, sections were washed and incubated 5 min with Hoechst solution 2 μg/mL as a nuclear counter-staining. Then, brain sections were washed and fixed with 4% paraformaldehyde. FLICA reagent is highly sensitive to specifically detect cells with activated caspases compared with other methods (Kaiser *et al.* 2008; Sekiya *et al.* 2005).

Morphometric analysis

In order to ensure objectivity, all measurements were performed on coded slices and were done separately by two different observers showing no significant differences between the results obtained by each. Mean gray level of S100B immunostained astroglial cells, morphometric parameters of GFAP stained astrocytes, MAP-2 and Nf-200 stained neurons and cell counts were performed using the NIH Image J software. Images taken with the microscope were captured with the digital camera, transformed to 8-bits gray scale, normalized and an interactive threshold selection was carried out. Once the threshold was determined it was kept fixed for the entire experiment. Following the threshold selection, the identification of the structures was performed using the software and indicating the maximal and minimal size of the expected structures (cells). Images of partial cells were excluded from all the counting processes. Astrocytes and neurons were randomly selected for the analysis, however only astrocytes showing the projections and a well defined soma were considered for the analysis. Then, the measurement of mean gray level (S100B immunostaining) and area parameters (GFAP, MAP-2 and Nf-200 immunostaining) were performed. Relative optical density (ROD) for the evaluation of S100B immunostaining intensity was obtained after a transformation of mean gray values into ROD by using the formula: ROD = log (256/mean gray) as was previously described (Ramos *et al.* 2000, 2004). A background parameter was obtained from each section out of the immunolabelled structures and subtracted from each cell ROD before

statistically processing values. For the analysis of neuronal alterations and NeuN staining, the counting was done manually discriminating the type of labeling observed in the neuronal nuclei. In all cases (neuronal or glial markers), approximately 10–15 fields per tissue section per treatment (C, IH-1; IH-3; IH-5; IH-10) per anatomical area (hippocampus, cortex) and marker were analyzed. The sections coming from six to eight animals per treatment were analyzed. Experiments and measurement were done 3–4 times showing identical results. The data were normalized and presented as pooled data in the graph. Statistical comparisons were analyzed with One-Way ANOVA and Student-Newman-Keuls post-test using Graph Pad Software (GraphPad Software Inc., San Diego, CA, USA).

The morphometric analysis of neurons and glial cells were focused in brain cortical layers IV–V and hippocampal CA1 region which are anatomical areas previously related to the cognitive impairment observed in experimental models of intermittent hypoxia and in sleep apnea human patients (Engleman *et al.* 2000; Décary *et al.* 2000; Gozal and Kheirandish-Gozal 2006). Neurogenic niches of SVZ and DG were analyzed with markers of glial cell division or immature astrocytes (PCNA and Vimentin respectively) (Valero *et al.* 2004).

Sholl analysis of astroglial projections

The Sholl analysis was performed as described in previous reports for dendritic arborization in neurons and oligondendrocyte branching (see for example Sholl 1953; Murtie *et al.* 2007; Campaña *et al.* 2008). Briefly, images of hippocampal or cortical GFAP stained astrocytes showing the soma and projections were processed as stated above, isolated with Adobe Photoshop software, digitized into binary morphology and skeletonized with the ImageJ NIH software (NIH, Bethesda, MD, USA). Thereafter, the analysis was performed with the ImageJ NIH plugin for Sholl analysis using nine concentric circles ranging from 2.5 to 25 μm from the center of astrocytic cell body, a distance enough to count most astroglial projections and presents an acceptable degree of overlapping with neighbor astrocytes (Fig. S1a). The astrocytic branching was evaluated in a minimum of 30 astrocytes per treatment and anatomical area per animal. The results from four animals per treatment were normalized and pooled for graphical presentation and statistical analysis.

Results

IH exposure induces a time-dependent reactive astrogliosis

Astrocytes from IH exposed animals showed larger projections and increased soma size as well as increased GFAP immunostaining, features typical of astroglial hypertrophy (Fig. 1a). The increased size of astrocytes was shown by the quantitative studies of the fraction area occupied by GFAP+ astrocytes that revealed an increase from IH-1 to IH-10 in hippocampus and parietal cortex (Fig. 1b). To confirm the changes in astrocytic morphology, a Sholl analysis was performed on the GFAP stained astrocytes. This showed that the number of projections extending from the center of astrocytic cell body was increased in the IH-exposed animals in hippocampus and brain cortex (Fig. 1c).

In animals exposed to IH, we observed an absolute increase in the number of GFAP+ astrocytes per field from IH-1 to IH-10 animals both in cerebral cortical layers IV–V and hippocampal CA-1 areas (Fig. 1d). To determine if the increased number of GFAP+ astrocytes corresponds to astrocytic cell division, vimentin expression was analyzed. Vimentin immunostaining, typically observed in immature astrocytes, was absent in glial cells from CA1 region of the hippocampus and in brain cortex (data not shown) and proliferating cell nuclear antigen (PCNA) immunostaining was not increased in GFAP+ astrocytes from IH-exposed animals (Fig. 1e). However, vimentin expression was increased in the neurogenic niches of DG and SVZ (Fig. 1f). Increased number of vimentin+ glial cells was also observed in the corpus callosum (Fig. 1f). Nestin expression was not increased in the SVZ and DG of the IH-exposed animals (data not shown).

Increased expression of S100B in astrocytes and RAGE expression in neurons after IH

Intermittent hypoxia exposed animals showed increased expression of the glial derived trophic factor S100B from IH-1 to IH-10, both in cortical and in hippocampal astrocytes (Fig. 2a). While control animals have populations of dense and weakly-stained S100B+ astrocytes, IH-exposed animals only showed dense S100B staining (Fig. 2a). The increased S100B content in astrocytes of these IH-exposed animals was also reflected by the statistical comparison of the optical density parameter that showed a maximal increase in IH-1 and IH-3 animals that persisted until IH-10 (Fig. 2b).

In IH exposed animals, double staining studies using GFAP/S100B showed the same alterations previously observed with GFAP or S100B stainings alone and there were no statistically significant changes in S100B-GFAP coexpression (data not shown). As RAGE seems to be essential for S100B action on neuronal survival (Huttunen *et al.* 2000; Kögel *et al.* 2004), RAGE expression was analyzed. RAGE immunostaining was not present in control animals but it appeared at IH-1 and IH-3 showing a dotted pattern that surrounded neuronal soma in brain cortical neurons (Fig. 2c). In hippocampus, RAGE dotted staining was also evidenced in the pyramidal cell layer from CA-1 and CA-2/3 and some pyramidal neurons showed a dense cytoplasmic RAGE expression (Fig. 2c). Quantitative studies showed that RAGE expression is increased in IH-1 and IH-3 groups and decreased by IH-10 (Fig. 2d). Double staining with RAGE/GFAP did not reveal astrocytes labeled for RAGE (data not shown).

Pyramidal neurons from hippocampus and cortical neurons are altered after IH exposure

Changes in neuronal nuclear morphology can be used to detect early signs of neuronal degeneration (Robertson *et al.*

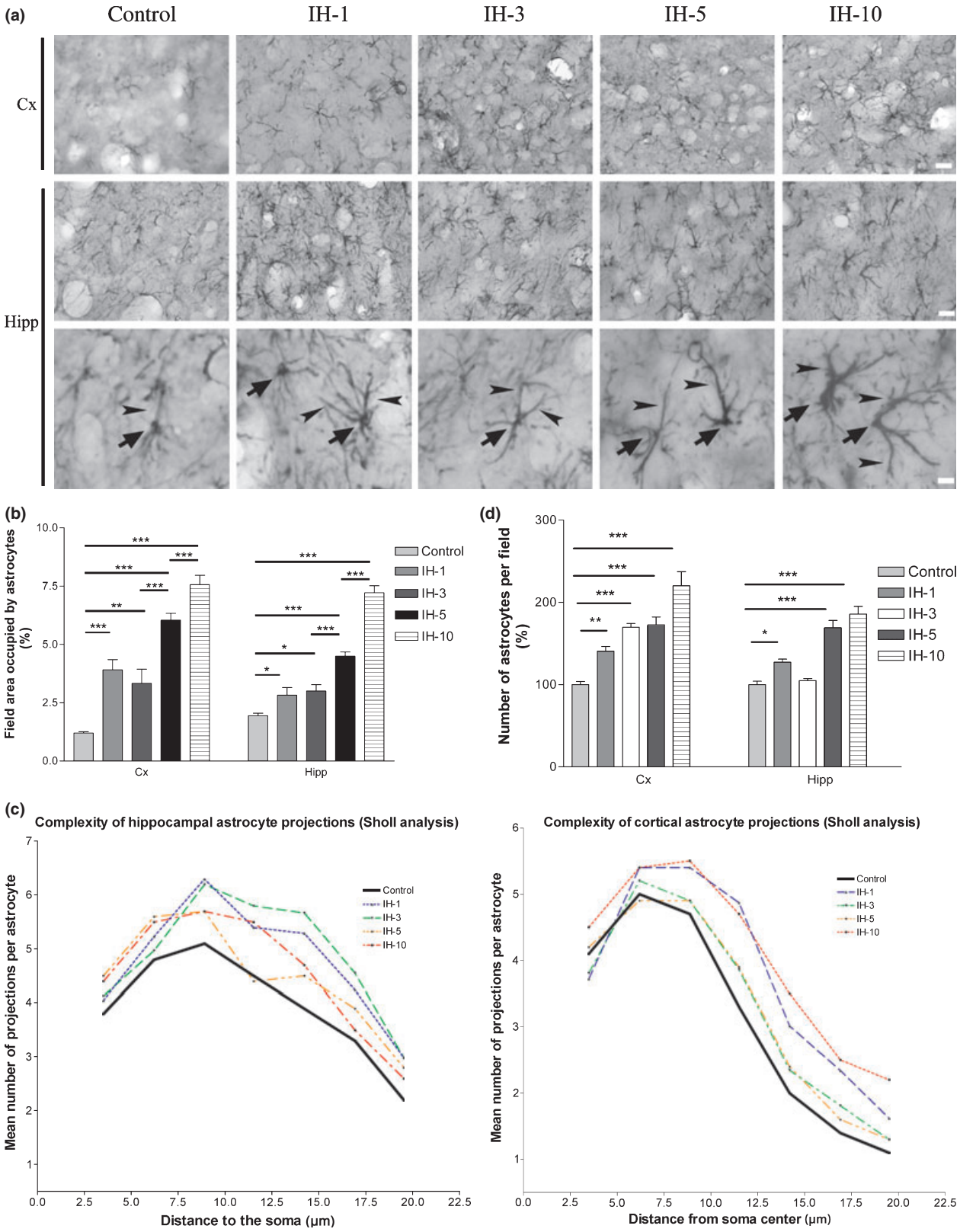

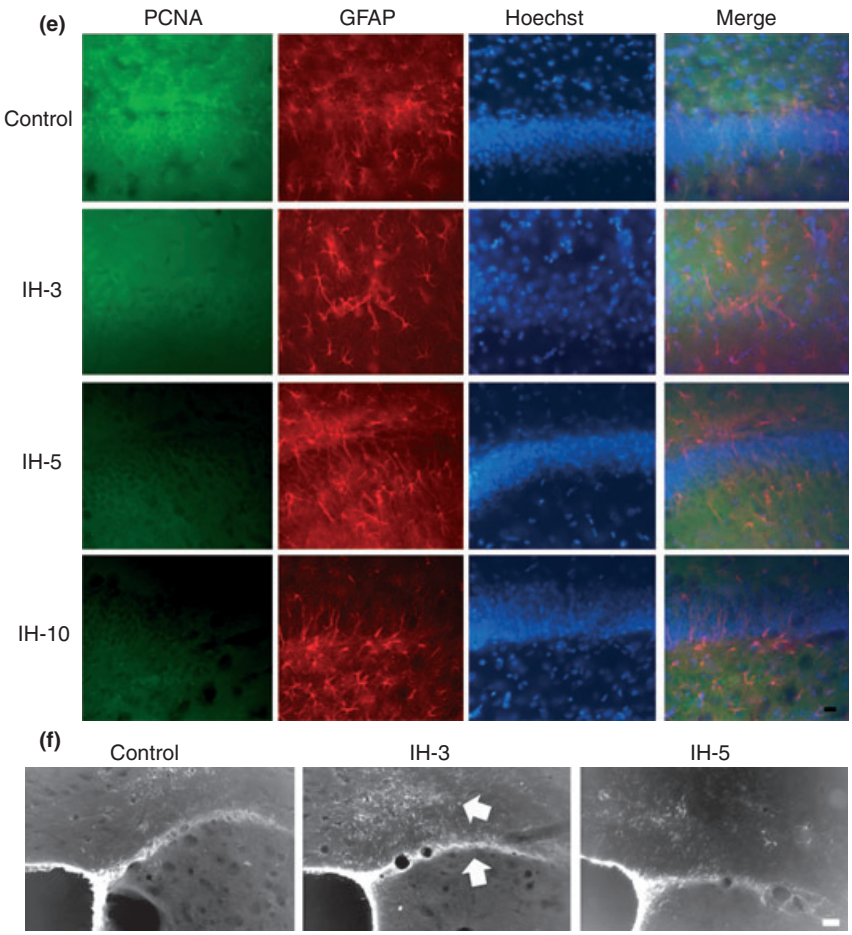

Fig. 1 (*Continued*).

2006). After IH, we observed that control animals presented normal neurons with intense nuclear NeuN staining, visible negative stained nucleolus and light NeuN+ cytoplasm while IH animals showed a large number of hippocampal and cortical pyramidal neurons with atypical dotted spongiform nuclear NeuN staining or even complete absence of NeuN nuclear staining with a redistribution of this protein to the cytoplasm (Fig. 3a). These alterations were observed most dramatically in brain cortex (layers IV–V) and CA-1 hippocampal neurons (Fig. 3a) of IH-3 animals. A quantification of these three subpopulations of NeuN+ neurons was performed by dividing the NeuN+ population in three categories: normal staining (intense NeuN+ nucleus plus light cytoplasm), sponge (spongiform nuclear NeuN+ staining) and cytoplasm (only cytoplasmic staining with nuclear NeuN negligible staining). The results indicated a significant increase in altered neurons at IH-3 and a reduction in the number of altered neurons at IH-5 and IH-10 (Fig. 3b). The

Fig. 1 (a) Representative photographs of GFAP immunostaining showing the astrocytic morphology in brain cortex (Cx), and hippocampal CA-1 area (Hipp). Note the distinctive features of reactive gliosis in IH exposed animals: increased astroglial cell area with increased soma size (arrows) and enlarged projections (arrowheads) in the IH-exposed animals, bar = 10 μm (upper panel); bar = 3.5 μm (lower panel). (b) Quantitative analysis of the field area covered by astrocytes showing the increase in the area occupied by astrocytes, data represent the percentage of microscopic field occupied by astrocytes. (c) Sholl analysis of astroglial GFAP-immunostained cells showing the number of projections per astrocyte at different distances from the centre of cell body; data represent the absolute number of projections at each distance. (d) Quantitative analysis of the number of GFAP-immunoreactive astrocytes per field in brain parietal cortex (Cx) and hippocampal CA-1 area (Hipp) after 1, 3, 5, 10 days of IH exposure, data represent the percentage of control. (e) Triple staining showing PCNA expression in GFAP+ astrocytes counter-stained with nuclear dye Hoechst 33342; note that PCNA expression was not increased in IH-exposed animals, bar = 10 μm. (f) Vimentin expression was increased in the neurogenic subventricular zone (SVZ) after IH exposure; arrows indicate the SVZ and the neighbouring area of the corpus callosum that presented increased number of Vim+ cells, bar = 30 μm. Data on the graphs represent the mean of the parameter in each condition, error bars represent the SEM. Significance between treatments was evaluated by one-way ANOVA and Student-Newman-Keuls post-test, $***p < 0.001$; $**p < 0.01$; $*p < 0.05$. Overall significance in Sholl analysis was tested by one-way ANOVA ($p < 0.05$), error bars are not represented to improve qualitative visualization of astrocytic morphometrical features.

total number of NeuN+ neurons trended downward from IH-1 to IH-10 but this apparent decrease did not reach statistical significance (Fig. 3c).

To confirm if the altered NeuN staining correlates with neuronal injury, active caspases were detected with Caspatag, a fluorescent inhibitor of caspases (FLICA) that

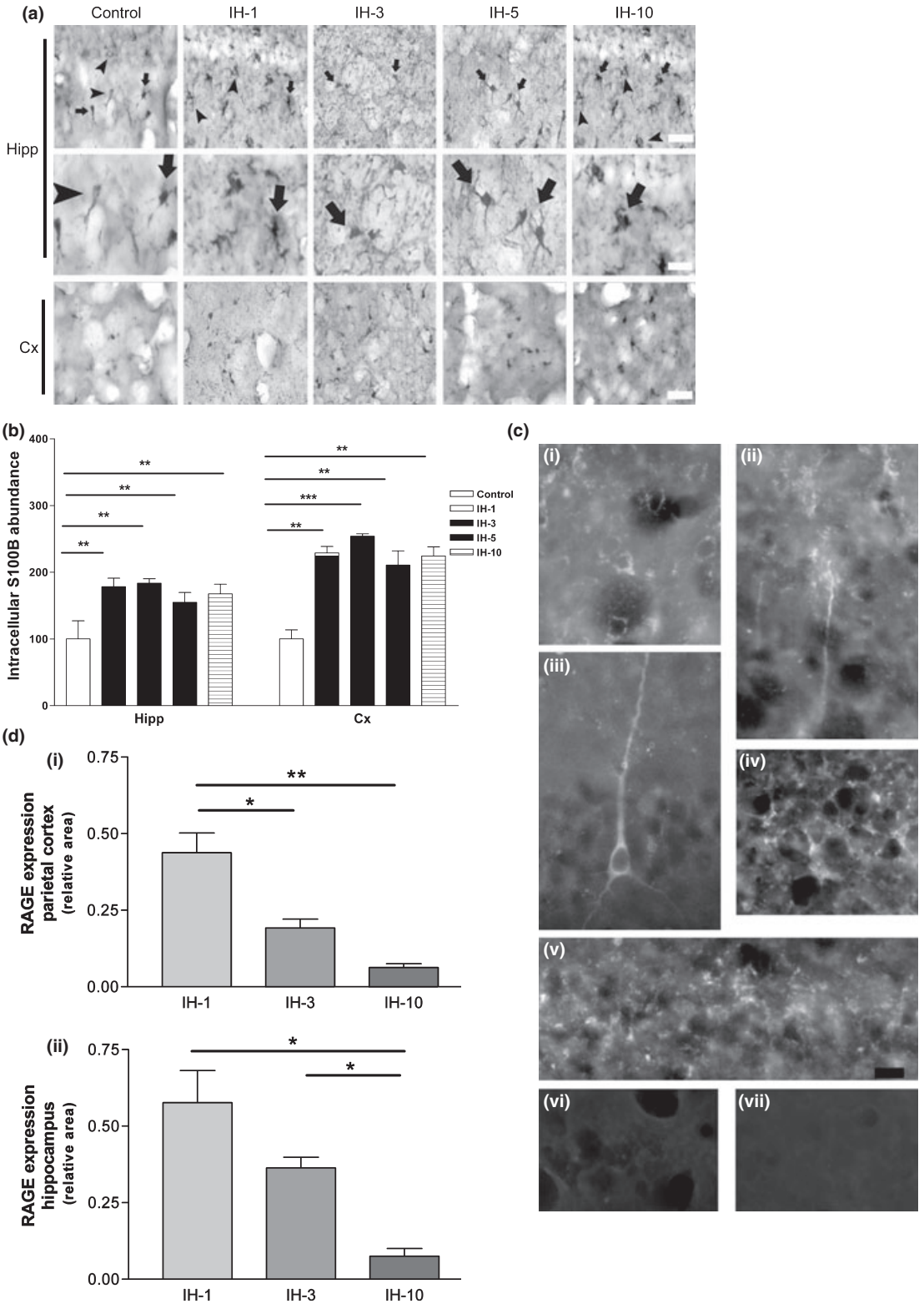

irreversibly binds to the active site of active caspases with high specificity (Sekiya *et al.* 2005; Kaiser *et al.* 2008). Figure 3(d) shows that Caspatag staining was associated with the IH-3 group; these same neurons presented altered NeuN staining with atypical nuclear morphology and we conclude that neurons in these regions undergo programmed cell death. In addition to Caspatag detection, nuclear morphology and neuronal identity were verified with Hoeschst and NeuN colabelling to identify neurons undergoing degeneration. The results showed that neurons with active caspases were mainly present in the IH-3 group and presented altered NeuN staining with atypical nuclear morphology (Fig. 3d).

Neuronal dendrites are also sensitive to neuronal stress and they present morphological alterations even under sublethal hypoxic conditions (Park *et al.* 1996). Time-dependent changes in the dendrite morphology were analyzed using MAP-2, a dendrite-specific marker. MAP-2 immunostaining showed significant alterations in dendrite morphology of pyramidal neurons in the hippocampal CA-1 area especially in the IH-3 group, where disruption of NeuN staining and active caspases were observed. Dendrites were shorter and presented atypical rounded shape structures (Fig. 4a) similar to those described in cell cultures exposed to hypoxia (Park *et al.* 1996). Surprisingly, the IH-10 group showed essentially normal dendritic morphology that was confirmed by morphometric analysis showing the mean length of the longest dendrites (Fig. 4b). In order to confirm the alterations in neuronal cytoskeleton, the profile of neurofilament expression was evaluated in the IH-exposed animals. Neurofilament 200 kDa morphological alterations have been related to neurodegenerative processes (Julien and Mushynski 1998; Ramos *et al.* 2000). A similar result compared to MAP-2 was obtained when mature Neurofilament-200 kDa immunostaining was analyzed. Nf-200 kDa showed in IH-3 and IH-5 animals an increased number of neuronal cytoskeleton alterations and shortened neuronal projections especially in the apical dendrites of cortical pyramidal neurons and dendrites of stratum radiatum in the CA-1 hippocampal area (Fig. 4c). The quantification of area occupied by Nf-200 kDa+ projections clearly showed a reduction in IH-3 group and a subsequent recovery (Fig. 4d). Light neurofilament (Nf-68 kDa) expression, usually very low and increased in processes involving remodeling and plasticity (Ramos *et al.* 2000; Craveiro *et al.* 2008), was detected in IH-5 animals (Fig. 4e).

IH exposure induces the expression of transcription factor HIF-1α and the downstream gene mdr-1

After IH exposure, nuclear HIF-1α staining was dramatically increased in both the hippocampus and cortex (Fig. 5a). Double immunostaining studies showed that the HIF-1α increase occurred in neurons of the CA1 region of the hippocampus and cortical neurons (Fig. 5b). Quantitative studies demonstrated a time-dependence in the increased abundance of HIF-1α in hippocampus and brain cortex of IH-exposed animals (Fig. 5c). To confirm that the HIF-1α produced under these circumstances was functional, we also performed immunostaining for MDR-1, a HIF-1α target gene (Comerford *et al.* 2002; Wartenberg *et al.* 2003). Figure 5(d) shows that MDR-1 expression profile was essentially identical to that for HIF-1α.

Discussion

Experimental studies on rodents using IH exposure to mimic human SA are widely accepted models for analyzing the neurobiological basis of cognitive alterations observed in human SA (Gozal and Kheirandish-Gozal 2007; Row 2007). Structural alterations and changes in the neuro-glial interactions in brains of IH-exposed animals may provide the biological substrate to understand the anatomical and biochemical basis of neurocognitive deficits observed in human subjects.

Reactive gliosis, also named reactive astrogliosis or astroglial reaction, is a key component of the cellular response to CNS injury and comprises astroglial hypertrophy and hyperplasia (see for review Ridet *et al.* 1997; Stoll *et al.* 1998). The transition from the quiescent to the reactive astrocytic state is accompanied by an increase in intermediate filaments, predominantly GFAP, leading to an increase in the soma size and processes which is characterized as hypertrophy (Ramos *et al.* 2004; Schiffer *et al.* 1996; Stoll *et al.* 1998). Hyperplasia is an absolute increase in the number of

Fig. 2 (a) Representative photographs of S100B immunostaining showing the expression of the glial soluble factor S100B in astrocytes from brain cortex (Cx) and hippocampal CA-1 area (Hipp). Note the different populations of S100B immunolabeled astrocytes that were present in the IH-exposed animals with clear S100B+ cytoplasm (arrow head) and dark S100B+ cytoplasm (arrow). Increased S100B expression resulted in a larger number of dark S100B+ astrocytes in IH exposed animals, bar = 20 μm (upper and lower rows), bar = 10 μm (middle row). (b) Quantitative analysis of the intensity of S100B immunostaining expressed as percentage of the optical density in control animals. (c) RAGE expression was detected in cortical (i,ii) and hippocampal CA-1 neurons (iii,iv,v) in IH-exposed animals but not in the hippocampus (vi) and cortex (vii) of control animals; bar = 10 μm. (d) Quantitative analysis of RAGE expression in brain cortex (i) and hippocampal CA-1 (ii) showing the relative area occupied by RAGE+ neurons and neuronal projections. The area RAGE+ was related to the total area of the field in the cortical sections (216 × 162 μm at 40× primary magnification) or to the total area of the hippocampal CA-1 pyramidal cell layer. Data on the graphs represent the mean of the indicated parameter, error bars represent the SEM. Significance between treatments was evaluated by one-way ANOVA and Student-Newman-Keuls post-test, ***$p < 0.001$; **$p < 0.01$; *$p < 0.05$.

astrocytes because of increased cell division *in situ* or migration from neurogenic niches (Yan *et al.* 2009; Yang *et al.* 2009).

Our results showed that astrocytes respond to IH exposure with reactive gliosis after only one day of IH exposure. Hypertrophied astrocytes with larger soma size, augmented branching and increased GFAP expression were observed from IH-1 to IH-10. Hippocampal and cortical astrocytes responded with the same profile when the basal morphological differences between astrocytes from these areas were

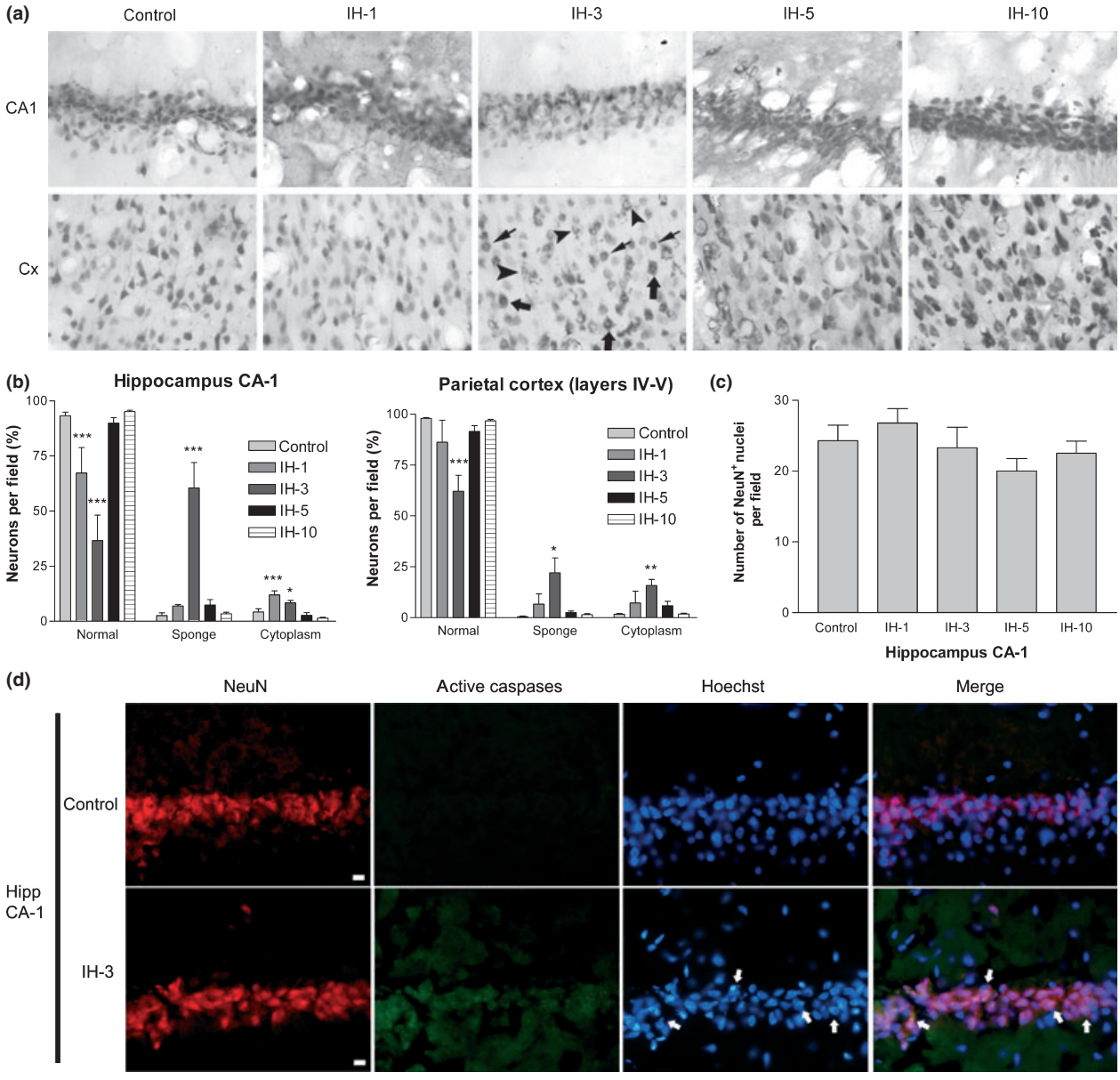

Fig. 3 (a) NeuN immunostaining shows the images of normal neuronal nuclei (thin arrows) in the hippocampal CA-1 area (CA-1) and brain cortex (layers IV–V) (Cx). Especially in IH-exposed animals increased cytoplasmic NeuN staining (thick arrows) was observed as well as atypical spongiform staining (arrow head) together with a number of neurons showing normal NeuN staining (thin arrows), bar = 10 μm. (b) Quantification of the different types of NeuN staining showed the maximal number of altered nuclei (spongiform or cytoplasmic-only NeuN) in IH-3 group, results are presented as percentage of NeuN+ cells per field. (c) Quantitative studies showing the absolute total number of NeuN+ cells per field, data are presented as total NeuN+ cells per field. (d) Triple staining with NeuN (red), active caspases (green) and nuclear staining (blue) showed increased caspases activation, arrows indicate apoptotic neurons. Data on the graphs represent the mean of each parameter ± SEM. Significance between treatments was evaluated by one-way ANOVA and Student-Newman-Keuls post-test, ***$p < 0.001$; **$p < 0.01$; *$p < 0.05$.

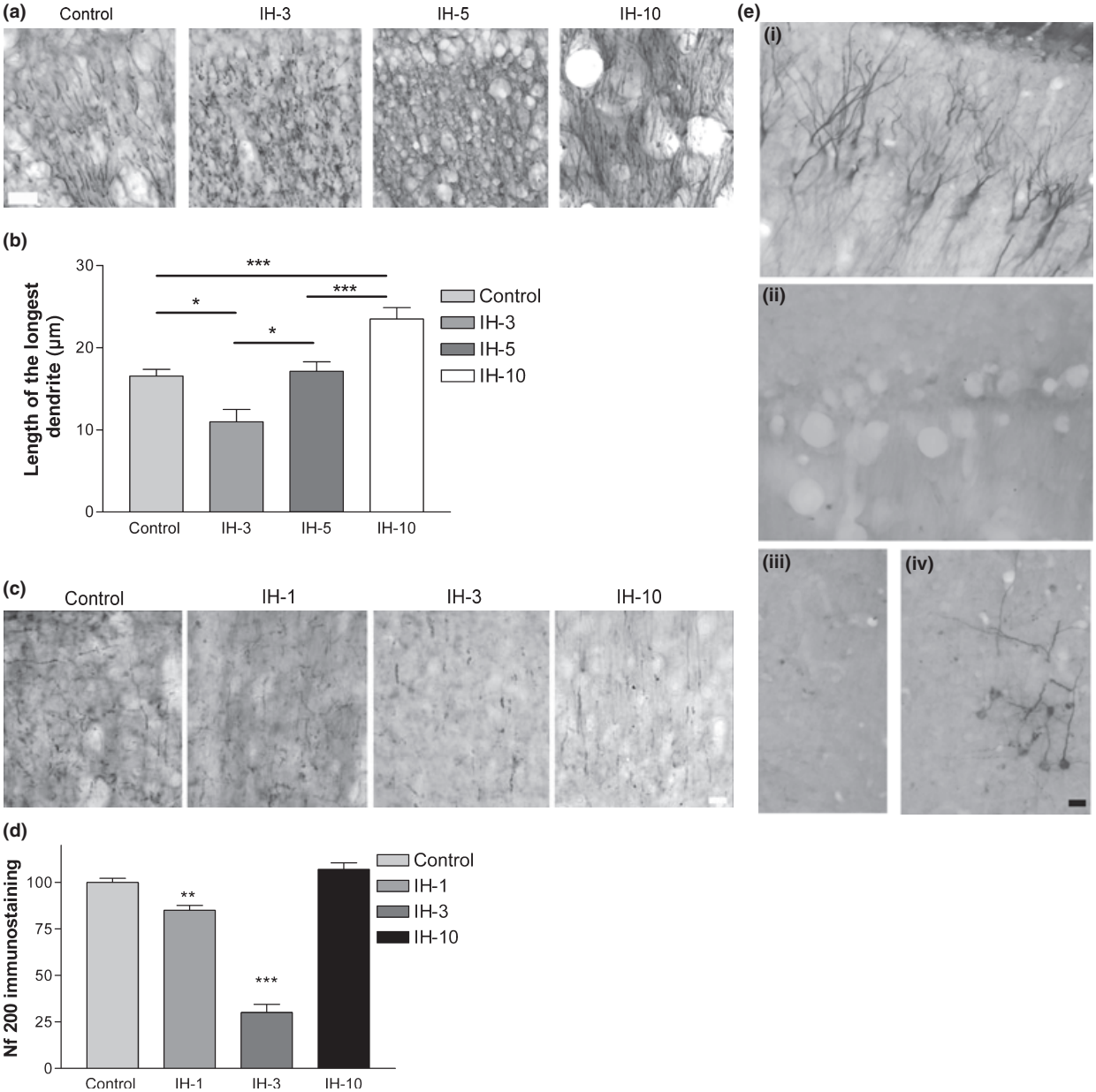

Fig. 4 (a) MAP-2 immunostaining in the hippocampal CA-1 area (stratum radiatum) showing a decrease in dendritic arborization in IH-3 and a recovery from IH-5 to IH-10 animals, bar = 10 μm. (b) Quantitative study showing the changes in dendrite length represented as the maximal dendrite length in the analyzed sections stained with MAP-2 antibodies. (c) Neurofilament 200 kDa immunostaining in hippocampus showing a decrease in the number and complexity of neuronal projections, bar = 10 μm. (d) Quantitative evaluation of Nf-200 kDa staining in the parietal cortex of IH-exposed animals. (e) Neurofilament 68 kDa expression in the hippocampal CA-1 (i,ii) and parietal cortex (iii,iv). The Nf-68 kDa increases in the IH-5 group (i,iv) while control animals have a low Nf-68 kDa expression (ii,iii), bar = 20 μm. Data on the graphs represent the mean of the parameter in each condition ± SEM. Significance between treatments was evaluated by one-way ANOVA and Student-Newman-Keuls post-test, ***$p < 0.001$; **$p < 0.01$; *$p < 0.05$.

considered. Astroglial hypertrophy was studied by Sholl analysis, a method that evaluates the number of projections at different distances from the astrocytic soma (Sholl 1953; Murtie *et al.* 2007; Campaña *et al.* 2008). Sholl analysis showed that the number of projections per astrocyte was increased at all evaluated time points of IH exposure. Our results demonstrate that astrocytes respond to IH faster than was previously reported by Gozal *et al.* (2001), where they showed images of hypertrophied GFAP-immunoreactive astrocytes after 14 days of IH. The reactive gliosis in that report was not followed by a time course profile from earlier time points and thus we consider that our results basically

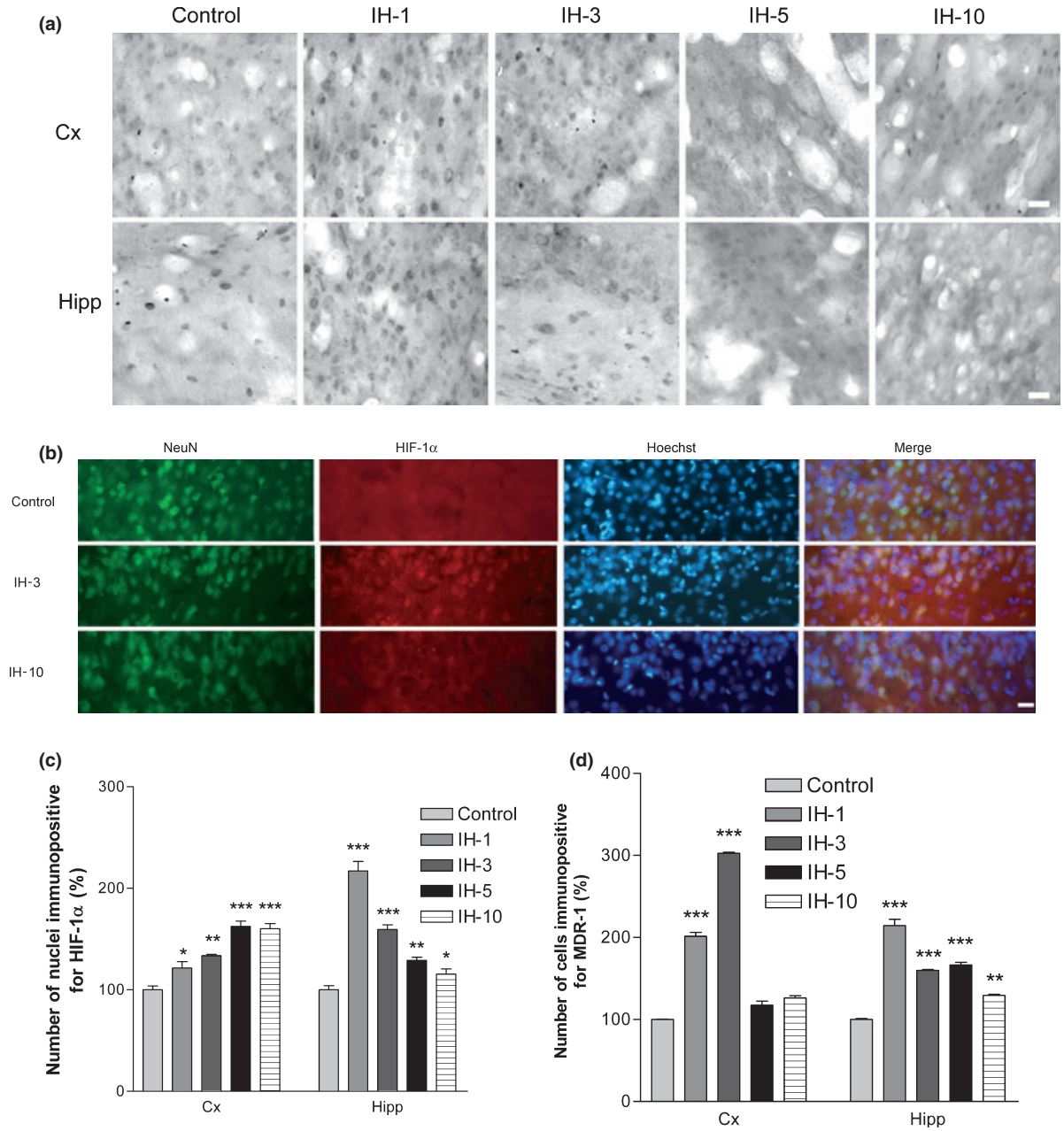

Fig. 5 (a) HIF-1α immunostaining in brain cortex (Cx) and hippocampal CA-1 area (Hipp) showing the increased nuclear staining of this transcription factor induced by the IH exposure, bar = 20 μm. (b) Double immunostaining showing HIF-1α and NeuN co-expression in the brain cortex indicating that HIF-1α abundance was increased in NeuN+ neurons in IH-3 and IH-10 groups, bar = 20 μm. (c) Quantification of the number of nuclei labelled with anti-HIF-1α in hippocampus CA-1 (Hipp) and brain cortex (Cx). **(d)** Quantification of MDR-1 immunolabeled cells in brain cortex (Cx) and hippocampus (Hipp). Data on the graphs represent the number of immunolabeled nuclei (HIF-1α) or cells (MDR-1) per field in each condition ± SEM. Significance between treatments was evaluated by one-way ANOVA and Student-Newman-Keuls post-test, $^{***}p < 0.001$; $^{**}p < 0.01$; $^{*}p < 0.05$.

demonstrate that reactive gliosis is an early cellular response to IH and persist during the IH exposure.

The IH exposure also induced an increase in the number of GFAP+ astrocytes per field from IH-1 to IH-10 animals (Fig. 6). The extent of the response was similar in brain cortex and hippocampus. This increase in GFAP+ astrocytes suggests that astroglial hyperplasia is occurring but neither Vimentin, a marker of immature or *newborn* astrocytes, or PCNA, a marker of cell division, were increased in hippocampal CA-1 or brain cortex of IH-exposed animals. Therefore, we believe it is more likely that the increase in GFAP+ cells reflects increased GFAP expression that is

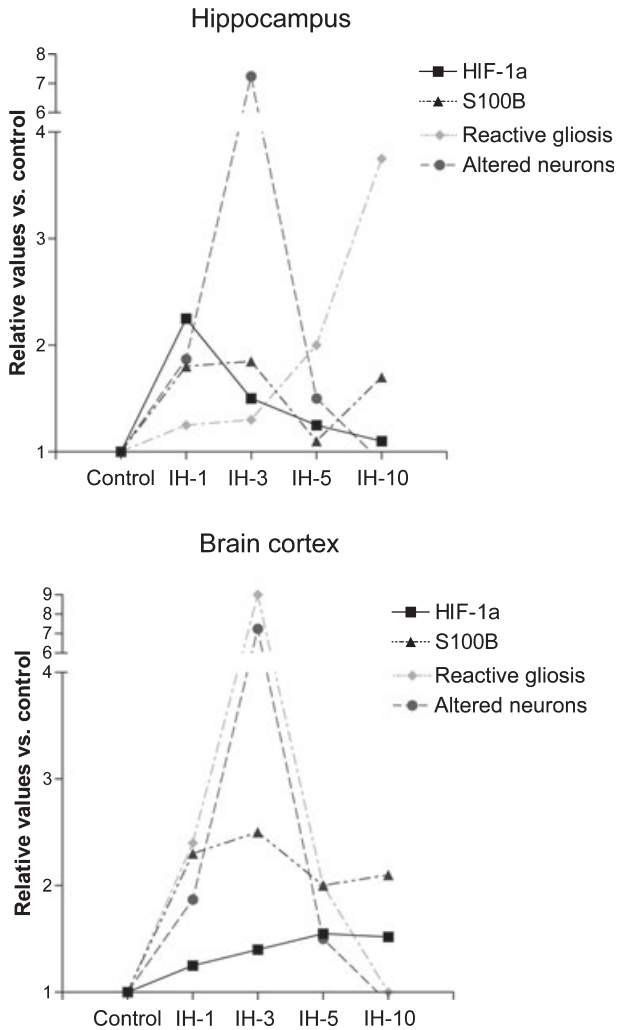

Fig. 6 Representation of the time-course changes in the reactive gliosis, neuronal alterations, S100B expression and HIF-1α abundance during the cycles of intermittent hypoxia in hippocampus (a) and parietal cortex (b). Data are presented as times of the values obtained for animals breathing normoxic room air (control).

induced by reactive gliosis. Note that we did detect a significant increase in the absolute number of Vimentin+ cells in neurogenic niches (SVZ and DG) and in Corpus Callosum thus demonstrating increased glial progenitors activity. In addition, a recent report also showed increased number of GFAP+ glial cells in cortex after IH that is reduced by antioxidant treatment (Burckhardt *et al.* 2008). In this scenario, a tempting hypothesis is that these increased activity in neurogenic niches and Corpus Callosum may provide the *new* astrocytes. In fact, SVZ activation by intermittent hypoxia was previously observed by bromodeoxyuridine (BrdU) staining but related to neurogenesis and not to gliogenesis in spite that no specific neural or glial markers were used in that early report (Zhu *et al.* 2005). Obviously, further studies are necessary to determine the origin and potential migration pathway that may provide astrocytes to cortex and hippocampus. In our hands, IH exposure induced an early astroglial response, suggesting that astroglial cells act as sensors of neuronal environment and establish a response to the IH exposure. Reactive gliosis in human SA occurs in the brainstem of children victims of sudden infant death syndrome that involved sleep apnea (Sawaguchi *et al.* 2003). It is proposed that reactive gliosis has a role in the determination of neuronal fate in SA as astrocytes can play a dual role, promoting neuronal survival by secreting trophic factors and removing harmful compounds versus facilitating neuronal death by promoting inflammation (Stoll *et al.* 1998; Ridet *et al.* 1997; Privat 2003). The glial protein S100B that is secreted by reactive astrocytes (Davey *et al.* 2001; Gerlach *et al.* 2006) is a molecule that has a dual role depending on the concentration inducing neuronal survival or death. In the nanomolar range of concentration S100B has a potent effect on neurite extension and enhances neuronal survival after injury while in the micromolar range S100B induces apoptotic neuronal death (Huttunen *et al.* 2000; Donato 2003; Ramos *et al.* 2004). S100B binds to the receptor for advanced end glycated products (RAGE), ultimately leading to the activation of NFκB signaling which seems to be the final output in this pathway (Huttunen *et al.* 2000; Kögel *et al.* 2004; Ponath *et al.* 2007). Our results in IH exposed animals showed that astrocytes had a significant early increase in the S100B expression in cortex and hippocampus that remained elevated until IH-10. These results support clinical observations that have shown increased level of S100B in peripheral blood of SA patients (Braga *et al.* 2006). Interestingly, the expression of RAGE, the proposed S100B receptor, was observed in a subset of pyramidal neurons from brain cortex and hippocampus of IH-1 and IH-3 animals. Therefore, the S100B-RAGE interaction could have an important role promoting neuronal death or survival in these areas. It is noteworthy that RAGE is expressed in the population of neurons from areas directly involved in the cognitive impairment in SA, that activation of NFκB is recognized as a main early response to IH (Xu *et al.* 2004) and that NFκB-induced transcription is a well known effect of RAGE activation by S100B (Donato 2003; Wang *et al.* 2007; Kögel *et al.* 2004).

Alterations in the expression and nuclear localization of the neuronal nuclear marker NeuN is an early event leading to neuronal degeneration (Robertson *et al.* 2006). In IH exposed animals we observed abnormal NeuN staining in a large number of hippocampal and cortical pyramidal neurons, especially in the IH-1 and IH-3 groups. These abnormal NeuN profiles were drastically diminished in IH-5 and IH-10 groups. The overall number of NeuN+ neurons trended downward from IH-1 to IH-10, possibly reflecting neuronal loss induced by IH exposure. Consistent with this, active caspases were identified in neurons showing an abnormal

NeuN profile and together, these observations are in accordance with previous reports of neuronal degeneration and programmed cell death after the exposure to IH (Gozal *et al.* 2001; Xu *et al.* 2004; Maiti *et al.* 2007). We found that neuronal cytoskeleton and dendritic projections were also altered by IH exposure. MAP-2 specific staining for dendrites showed shortened dendrites and atypical structures after initial IH exposure and near normal dendrite length was observed at IH-10, suggesting that surviving neurons had adapted to the hypoxic environment. In addition, mature Nf-200 kDa neurofilament staining also reflected the same profile of alterations at early time points and subsequent recovery in IH-10 group. Nf-68 kDa is usually increased in remodeling processes and was increased in IH-5 animals. Together with previous data showing that experimental IH produces partial neuronal loss in cerebellum, in hippocampal CA-1 area and in prefrontal cortex (Maiti *et al.* 2007; Xu *et al.* 2004) and decreases animal performance in learning paradigms (Zhang *et al.* 2006), our findings suggest that acute IH has an early drastic effect on neuronal function but that with continued exposure, adaptation that supports continued neuronal function may occur, even in presence of a profuse reactive gliosis (Fig. 6).

In this scenario, the HIF-1α can be involved in the development of tolerance to the hypoxia. In normal tissue, HIF-1α is rapidly destroyed by the proteasome but during hypoxia, HIF-1α is stabilized and translocates into the nucleus where its binds HIF-1β and forms the active HIF-1 complex. The HIF complex activates genes directly related to the cell survival in conditions of hypoxia in the CNS (Helton *et al.* 2005; Vangeison *et al.* 2008; Semenza 2002a). Our results showed increased number of neurons with nuclear HIF-1α staining demonstrating that IH induces HIF-1α stabilization and migration to the nucleus, where is able to activate downstream genes as mdr-1 that we also detected in the IH exposed brains. MDR-1 is involved in the excretion of xenobiotics and toxic compounds from the cells and across the blood-brain barrier (Ramos *et al.* 2004; Lazarowski *et al.* 2007). Interestingly, RAGE is up-regulated in neurons in the area of the cortical infarct by a HIF-1α dependent mechanism (Pichiule *et al.* 2007) and therefore HIF-1α dependent gene transcription may have a major role in determining neuronal survival after IH and SA. However, HIF-1α may not be alone in determining neuronal survival after IH. Reactive gliosis should be also considered as reactive astrocytes secrete different molecules including S100B. S100B, acting on the RAGE receptor expressed by hippocampal and cortical neurons, may induce NFκB activation which, in turn, can improve neuronal survival in IH conditions.

The IH exposure paradigm used in our experiments draws on earlier rodent models and is consistent with the clinical definition of sleep apnea in that it provides at least five hypoxic events per hour of sleep [Basner 2007; Ma *et al.* 2008; Ling *et al.* 2008; Klein *et al.* 2005; Hinojosa-Laborde and Mifflin 2005). Interestingly, even this low number of IH cycles decreased the rats' oxygen hemoglobin saturation by 15–20%, increased heart rate by 20–30 beats/min, and produced significant neuronal and glial alterations in brain cortex and hippocampus. The importance of the progression and time-dependence of this early events that we studied with this mild paradigm is evidenced when we consider that programmed neuronal death is an early event in IH that peaks after 48 h of exposure (Gozal *et al.* 2001) and that glutamate excitotoxicity in hippocampus is promoted by a short number of cycles of IH exposure (Fung *et al.* 2007). The activity of key enzymes related to neuronal survival, such as Akt and glycogen synthase kinase 3 beta (GSK3β), show altered activity between 1 h and 3 days of IH exposure and then returned to baseline levels between 14 and 30 days of IH exposure (Goldbart *et al.* 2003a) supporting the idea of adaptation to the IH conditions. Transcription factors involved in IH stress response in neurons such as NFκB, c-*Jun* and c-*Fos* have also the maximal induction after 3 days of IH exposure (Xu *et al.* 2004). Thus we considered that it was necessary to study neuronal and glial alterations at early time points and reduce the number of IH cycles to improve our knowledge about this model of such an important human pathology as SA.

In summary, our data characterize early glial and neuronal response to IH in areas involved in the cognitive impairment observed in human patients suffering from SA (Fig. 6). Reactive astrogliosis, increased S100B levels, and neuronal expression of RAGE probably lie downstream of HIF-1α activation. Early neuronal alterations suggest an active role of S100B-RAGE in the consequences of IH. Significant adaptation to IH occurs at later time points, suggesting that tolerance and/or conditioning is triggered by IH. NFκB and HIF-1α transcriptional events are obvious, but not unique, candidates that may mediate the adaptation process triggered by IH exposure.

Acknowledgements

This work was supported by grants CONICET PIP6063 and PIP1728, PICT jovenes 33735/05, TWAS 04-370 RG/BIO/LA grant and an IBRO Return Home Fellowship. RXAR, MFA and AV are fellows from CONICET (Argentina). AJR and HR are researchers from CONICET (Argentina). We thank Dr. Phil Barker (MNI, McGill University, Canada) for the comments and help editing the manuscript.

Supporting Information

Additional Supporting Information may be found in the online version of this article:

Figure S1. Schematic representation of Sholl analysis.

As a service to our authors and readers, this journal provides supporting information supplied by the authors. Such materials are peer-reviewed and may be re-organized for online delivery, but are

not copy-edited or typeset. Technical support issues arising from supporting information (other than missing files) should be addressed to the authors.

References

Altay T., Gonzales E. R., Park T. S. and Gidday J. M. (2004) Cerebrovascular inflammation after brief episodic hypoxia: modulation by neuronal and endothelial nitric oxide synthase. *J. Appl. Physiol.* **96**(3), 1223–1230; discussion 1196.

Angelo M. F., Aviles-Reyes R. X., Villarreal A., Barker P., Reines A. G. and Ramos A. J. (2009) p75 NTR expression is induced in isolated neurons of the penumbra after ischemia by cortical devascularization. *J. Neurosci. Res.* **87**(8), 1892–1903.

Ayalon L. and Peterson S. (2007) Functional central nervous system imaging in the investigation of obstructive sleep apnea. *Curr. Opin. Pulm. Med.* **13**(6), 479–483.

Basner R. C. (2007) Continuous positive airway pressure for obstructive sleep apnea. *N. Engl. J. Med.* **356**(17), 1751–1758.

Bernhardt W. M., Warnecke C., Willam C., Tanaka T., Wiesener M. S. and Eckardt K. U. (2007) Organ protection by hypoxia and hypoxia-inducible factors. *Methods Enzymol.* **435**, 221–245.

Braga C. W., Martinez D., Wofchuk S., Portela L. V. and Souza D. O. (2006) S100B and NSE serum levels in obstructive sleep apnea syndrome. *Sleep Med.* **7**(5), 431–435.

Bravo M. de L., Serpero L. D., Barceló A., Barbé F., Agustí A. and Gozal D. (2007) Inflammatory proteins in patients with obstructive sleep apnea with and without daytime sleepiness. *Sleep Breath.* **11**(3), 177–185.

Burckhardt I. C., Gozal D., Dayyat E., Cheng Y., Li R. C., Goldbart A. D. and Row B. W. (2008) Green tea catechin polyphenols attenuate behavioral and oxidative responses to intermittent hypoxia. *Am. J. Respir. Crit. Care Med.* **177**(10), 1135–1141.

Campaña A. D., Sanchez F., Gamboa C., Gómez-Villalobos M. de J., De La Cruz F., Zamudio S. and Flores G. (2008) Dendritic morphology on neurons from prefrontal cortex, hippocampus, and nucleus accumbens is altered in adult male mice exposed to repeated low dose of malathion. *Synapse* **62**(4), 283–290.

Comerford K. M., Wallace T. J., Karhausen J., Louis N. A., Montalto M. C. and Colgan S. P. (2002) Hypoxia-inducible factor-1-dependent regulation of the multidrug resistance (MDR1) gene. *Cancer Res.* **62**(12), 3387–3394.

Craveiro L. M., Hakkoum D., Weinmann O., Montani L., Stoppini L. and Schwab M. E. (2008) Neutralization of the membrane protein Nogo-A enhances growth and reactive sprouting in established organotypic hippocampal slice cultures. *Eur. J. Neurosci.* **28**(9), 1808–1824.

Davey G. E., Murmann P. and Heizmann C. W. (2001) Intracellular Ca2+ and Zn2+ levels regulate the alternative cell density-dependent secretion of S100B in human glioblastoma cells. *J. Biol. Chem.* **276**(33), 30819–30826.

Décary A., Rouleau I. and Montplaisir J. (2000) Cognitive deficits associated with sleep apnea syndrome: a proposed neuropsychological test battery. *Sleep* **23**(3), 369–381.

Donato R. (2003) Intracellular and extracellular roles of S100 proteins. *Microsc. Res. Tech.* **60**(6), 540–551.

Engleman H. M., Kingshott R. N., Martin S. E. and Douglas N. J. (2000) Cognitive function in the sleep apnea/hypopnea syndrome (SAHS). *Sleep* **23**(Suppl. 4), S102–S108.

Feuerstein C., Naegelé B., Pépin J. L. and Lévy P. (1997) Frontal lobe-related cognitive functions in patients with sleep apnea syndrome before and after treatment. *Acta Neurol. Belg.* **97**(2), 96–107.

Fung S. J., Xi M. C., Zhang J. H., Sampogna S., Yamuy J., Morales F. R. and Chase M. H. (2007) Apnea promotes glutamate-induced excitotoxicity in hippocampal neurons. *Brain Res.* **1179**, 42–50.

Gerlach R., Demel G., König H. G., Gross U., Prehn J. H., Raabe A., Seifert V. and Kögel D. (2006) Active secretion of S100B from astrocytes during metabolic stress. *Neuroscience* **141**(4), 1697–1701.

Goldbart A., Cheng Z. J., Brittian K. R. and Gozal D. (2003a) Intermittent hypoxia induces time-dependent changes in the protein kinase B signaling pathway in the hippocampal CA1 region of the rat. *Neurobiol. Dis.* **14**(3), 440–446.

Gozal D. and Kheirandish-Gozal L. (2007) Neurocognitive and behavioral morbidity in children with sleep disorders. *Curr. Opin. Pulm. Med.* **13**(6), 505–509.

Gozal D. and Kheirandish-Gozal L. (2008) Cardiovascular morbidity in obstructive sleep apnea: oxidative stress, inflammation, and much more. *Am. J. Respir. Crit. Care Med.* **177**(4), 369–375.

Gozal D., Daniel J. M. and Dohanich G. P. (2001) Behavioral and anatomical correlates of chronic episodic hypoxia during sleep in the rat. *J. Neurosci.* **21**(7), 2442–2450.

Gozal E., Gozal D., Pierce W. M. *et al.* (2002) Proteomic analysis of CA1 and CA3 regions of rat hippocampus and differential susceptibility to intermittent hypoxia. *J. Neurochem.* **83**(2), 331–345.

Gozal D., Row B. W., Gozal E., Kheirandish L., Neville J. J., Brittian K. R., Sachleben L. R. Jr and Guo S. Z. (2003) Temporal aspects of spatial task performance during intermittent hypoxia in the rat: evidence for neurogenesis. *Eur. J. Neurosci.* **18**(8), 2335–2342.

Helton R., Cui J., Scheel J. R. *et al.* (2005) Brain-specific knock-out of hypoxia-inducible factor-1alpha reduces rather than increases hypoxic-ischemic damage. *J. Neurosci.* **25**(16), 4099–4107. Erratum in: *J. Neurosci.* 25(19):1 p following 4888.

Hinojosa-Laborde C. and Mifflin S. W. (2005) Sex differences in blood pressure response to intermittent hypoxia in rats. *Hypertension.* **46**(4), 1016–1021.

Hung M. W., Tipoe G. L., Poon A. M., Reiter R. J. and Fung M. L. (2008) Protective effect of melatonin against hippocampal injury of rats with intermittent hypoxia. *J. Pineal Res.* **44**(2), 214–221.

Huttunen H. J., Kuja-Panula J., Sorci G., Agneletti A. L., Donato R. and Rauvala H. (2000) Coregulation of neurite outgrowth and cell survival by amphoterin and S100 proteins through receptor for advanced glycation end products (RAGE) activation. *J. Biol. Chem.* **275**(51), 40096–40105.

Julien J. P. and Mushynski W. E. (1998) Neurofilaments in health and disease. *Prog. Nucleic Acid Res. Mol. Biol.* **61**, 1–23.

Kaiser C. L., Chapman B. J., Guidi J. L., Terry C. E., Mangiardi D. A. and Cotanche D. A. (2008) Comparison of activated caspase detection methods in the gentamicin treated chick cochlea. *Hear. Res.* **240**(1-2), 1–11.

Kheirandish-Gozal L. (2006) Practical aspects of scoring sleep in children. *Paediatr. Respir. Rev.* **7**(Suppl 1), S50–S54.

Klein J. B., Barati M. T., Wu R., Gozal D., Sachleben L. R. Jr, Kausar H., Trent J. O., Gozal E. and Rane M. J. (2005) Akt-mediated valosin-containing protein 97 phosphorylation regulates its association with ubiquitinated proteins. *J. Biol. Chem.* **280**(36), 31870–31881.

Kögel D., Peters M., König H. G., Hashemi S. M., Bui N. T., Arolt V., Rothermundt M. and Prehn J. H. (2004) S100B potently activates p65/c-Rel transcriptional complexes in hippocampal neurons: Clinical implications for the role of S100B in excitotoxic brain injury. *Neuroscience* **127**(4), 913–920.

Lavie L. (2003) Obstructive sleep apnoea syndrome-an oxidative stress disorder. *Sleep Med. Rev.* **7**(1), 35–51.

Lazarowski A., Caltana L., Merelli A., Rubio M. D., Ramos A. J. and Brusco A. (2007) Neuronal mdr-1 gene expression after experimental focal hypoxia: a new obstacle for neuroprotection? *J. Neurol. Sci.* **258**(1–2), 84–92.

Liberto C. M., Albrecht P. J., Herx L. M., Yong V. W. and Levison S. W. (2004) Pro-regenerative properties of cytokine-activated astrocytes. *J. Neurochem.* **89**(5), 1092–1100.

Ling Q., Sailan W., Ran J., Zhi S., Cen L., Yang X. and Xiaoqun Q. (2008) The effect of intermittent hypoxia on bodyweight, serum glucose and cholesterol in obesity mice. *Pak. J. Biol. Sci.* **11**(6), 869–875.

Lu G. W., Yu S., Li R. H., Cui X. Y. and Gao C. Y. (2005) Hypoxic preconditioning: a novel intrinsic cytoprotective strategy. *Mol. Neurobiol.* **31**(1–3), 255–271.

Ma S., Mifflin S. W., Cunningham J. T. and Morilak D. A. (2008) Chronic intermittent hypoxia sensitizes acute hypothalamic-pituitary-adrenal stress reactivity and Fos induction in the rat locus coeruleus in response to subsequent immobilization stress. *Neuroscience* **154**(4), 1639–1647.

Machaalani R. and Waters K. A. (2003) Increased neuronal cell death after intermittent hypercapnic hypoxia in the developing piglet brainstem. *Brain Res.* **985**(2), 127–134.

Maiti P., Singh S. B., Muthuraju S., Veleri S. and Ilavazhagan G. (2007) Hypobaric hypoxia damages the hippocampal pyramidal neurons in the rat brain. *Brain Res.* **1175**, 1–9.

Maragakis N. J. and Rothstein J. D. (2006) Mechanisms of disease: astrocytes in neurodegenerative disease. *Nat. Clin. Pract. Neurol.* **2**(12), 679–689.

Morrell M. J. and Twigg G. (2006) Neural consequences of sleep disordered breathing: the role of intermittent hypoxia. *Adv. Exp. Med. Biol.* **588**, 75–88.

Murtie J. C., Macklin W. B. and Corfas G. (2007) Morphometric analysis of oligodendrocytes in the adult mouse frontal cortex. *J. Neurosci. Res.* **85**(10), 2080–2086.

Naegele B., Pepin J. L., Levy P., Bonnet C., Pellat J. and Feuerstein C. (1998) Cognitive executive dysfunction in patients with obstructive sleep apnea syndrome (OSAS) after CPAP treatment. *Sleep* **21**(4), 392–397.

Nanduri J. and Nanduri R. P. (2007) Cellular mechanisms associated with intermittent hypoxia. *Essays Biochem.* **43**, 91–104.

Pae E. K., Chien P. and Harper R. M. (2005) Intermittent hypoxia damages cerebellar cortex and deep nuclei. *Neurosci. Lett.* **375**(2), 123–128.

Park J. S., Bateman M. C. and Goldberg M. P. (1996) Rapid alterations in dendrite morphology during sublethal hypoxia or glutamate receptor activation. *Neurobiol. Dis.* **3**(3), 215–227.

Payne R. S., Goldbart A., Gozal D. and Schurr A. (2004) Effect of intermittent hypoxia on long-term potentiation in rat hippocampal slices. *Brain Res.* **1029**(2), 195–199.

Pichiule P., Chavez J. C., Schmidt A. M. and Vannucci S. J. (2007) Hypoxia-inducible factor-1 mediates neuronal expression of the receptor for advanced glycation end products following hypoxia/ischemia. *J. Biol. Chem.* **282**(50), 36330–36340.

Ponath G., Schettler C., Kaestner F., Voigt B., Wentker D., Arolt V. and Rothermundt M. (2007) Autocrine S100B effects on astrocytes are mediated via RAGE. *J. Neuroimmunol.* **184**(1–2), 214–222.

Privat A. (2003) Astrocytes as support for axonal regeneration in the central nervous system of mammals. *Glia* **43**(1), 91–93.

Ramos A. J., Tagliaferro P., López E. M., Pecci Saavedra J. and Brusco A. (2000) Neuroglial interactions in a model of para-chlorophenylalanine-induced serotonin depletion. *Brain Res.* **883**(1), 1–14.

Ramos A. J., Rubio M. D., Defagot C., Hischberg L., Villar M. J. and Brusco A. (2004) The 5HT1A receptor agonist, 8-OH-DPAT, protects neurons and reduces astroglial reaction after ischemic damage caused by cortical devascularization. *Brain Res.* **1030**(2), 201–220.

Ridet J. L., Malhotra S. K., Privat A. and Gage F. H. (1997) Reactive astrocytes: cellular and molecular cues to biological function. *Trends Neurosci.* **20**(12), 570–577.

Robertson C. L., Puskar A., Hoffman G. E., Murphy A. Z., Saraswati M. and Fiskum G. (2006) Physiologic progesterone reduces mitochondrial dysfunction and hippocampal cell loss after traumatic brain injury in female rats. *Exp. Neurol.* **197**(1), 235–243.

Roure N., Gomez S., Mediano O. *et al.* (2008) Daytime sleepiness and polysomnography in obstructive sleep apnea patients. *Sleep Med* **9**(7), 727–731.

Row B. W. (2007) Intermittent hypoxia and cognitive function: implications from chronic animal models. *Adv. Exp. Med. Biol.* **618**, 51–67.

Row B. W., Kheirandish L., Neville J. J. and Gozal D. (2002) Impaired spatial learning and hyperactivity in developing rats exposed to intermittent hypoxia. *Pediatr. Res.* **52**(3), 449–453.

Row B. W., Liu R., Xu W., Kheirandish L. and Gozal D. (2003) Intermittent hypoxia is associated with oxidative stress and spatial learning deficits in the rat. *Am. J. Respir. Crit. Care Med.* **167**(11), 1548–1553.

Sawaguchi T., Patricia F., Kadhim H., Groswasser J., Sottiaux M., Nishida H. and Kahn A. (2003) Clinicopathological correlation between brainstem gliosis using GFAP as a marker and sleep apnea in the sudden infant death syndrome. *Early Hum. Dev.* **75**(Suppl), S3–S11.

Schiffer D., Cordera S., Cavalla P. and Migheli A. (1966) Reactive astrogliosis of the spinal cord in amyotrophic lateral sclerosis. *J. Neurol. Sci.* **139**(Suppl), 27–33.

Sekiya M., Funahashi H., Tsukamura K., Imai T., Hayakawa A., Kiuchi T. and Nakao A. (2005) Intracellular signaling in the induction of apoptosis in a human breast cancer cell line by water extract of Mekabu. *Int. J. Clin. Oncol.* **10**(2), 122–126.

Semenza G. L. (2002a) Involvement of hypoxia-inducible factor 1 in human cancer. *Intern. Med.* **41**(2), 79–83.

Semenza G. L. (2002b) HIF-1 and tumor progression: pathophysiology and therapeutics. *Trends. Mol. Med*. **8**(4 Suppl), S62–S67.

Sharp F. R. and Bernaudin M. (2004) HIF1 and oxygen sensing in the brain. *Nat. Rev. Neurosci.* **5**(6), 437–448.

Sharp F. R., Bergeron M. and Bernaudin M. (2001) Hypoxia-inducible factor in brain. *Adv. Exp. Med. Biol.* **502**, 273–291.

Sholl D. A. (1953) Dendritic organization in the neurons of the visual and motor cortices of the cat. *J. Anat.* **87**(4), 387–406.

Sizonenko S. V., Sirimanne E., Mayall Y., Gluckman P. D., Inder T. and Williams C. (2003) Selective cortical alteration after hypoxic-ischemic injury in the very immature rat brain. *Pediatr. Res.* **54**(2), 263–269.

Stoll G., Jander S. and Schroeter M. (1998) Inflammation and glial responses in ischemic brain lesions. *Prog. Neurobiol.* **56**(2), 149–171.

Thomas R. J., Rosen B. R., Stern C. E., Weiss J. W. and Kwong K. K. (2005) Functional imaging of working memory in obstructive sleep-disordered breathing. *J. Appl. Physiol.* **98**(6), 2226–2234.

Valero J., Weruaga E., Murias A. R., Porteros A. and Alonso J. R. (2004) Immunodetection of BrdU and PCNA in the rostral migratory stream of the adult mouse, in *Current Issues on Multidisciplinary Microscopy Research and Education, Vol. 2 of FORMATEX Microscopy Book Series* (Méndez-Vilas A. and Labajos-Broncano L., eds), pp. 118–129. Kluver-Formatex, Badajoz.

Vangeison G., Carr D., Federoff H. J. and Rempe D. A. (2008) The good, the bad, and the cell type-specific roles of hypoxia inducible factor-1 alpha in neurons and astrocytes. *J. Neurosci.* **28**(8), 1988–1993.

Wang L., Li S. and Jungalwala F. B. (2007) Receptor for advanced glycation end products (RAGE) mediates neuronal differentiation and neurite outgrowth. *J. Neurosci. Res.* **86**(6), 1254–1266.

Wartenberg M., Ling F. C., Müschen M. *et al.* (2003) Regulation of the multidrug resistance transporter P- glycoprotein in multicellular tumor spheroids by hypoxia-inducible factor (HIF-1) and reactive oxygen species. *FASEB J.* **17**(3), 503–505.

Xu W., Chi L., Row B. W. *et al.* (2004) Increased oxidative stress is associated with chronic intermittent hypoxia-mediated brain cortical neuronal cell apoptosis in a mouse model of sleep apnea. *Neuroscience* **126**(2), 313–323.

Yan Y. P., Lang B. T., Vemuganti R. and Dempsey R. J. (2009) Persistent migration of neuroblasts from the subventricular zone to the injured striatum mediated by osteopontin following intracerebral hemorrhage. *J. Neurochem.* **109**(6), 1624–1635.

Yang J., Liu J., Niu G., Chan K. C., Wang R., Liu Y. and Wu E. X. (2009) *In vivo* MRI of endogenous stem/progenitor cell migration from subventricular zone in normal and injured developing brains. *Neuroimage* **48**(2), 319–328.

Zhang J. X., Lu X. J., Wang X. C., Li W. and Du J. Z. (2006) Intermittent hypoxia impairs performance of adult mice in the two-way shuttle box but not in the Morris water maze. *J. Neurosci. Res.* **84**(1), 228–235.

Zhu L. L., Zhao T., Li H. S., Zhao H., Wu L. Y., Ding A. S., Fan W. H. and Fan M. (2005) Neurogenesis in the adult rat brain after intermittent hypoxia. *Brain Res.* **1055**(1–2), 1–6.

Zhu Y., Fenik P., Zhan G., Sanfillipo-Cohn B., Naidoo N. and Veasey S. C. (2008) Eif-2a protects brainstem motoneurons in a murine model of sleep apnea. *J. Neurosci.* **28**(9), 2168–2178.

